

Accurate determination of acceleration statistics in a turbulent jet using locally adapted TrackFit

T. Buchwald^{1*}, D. Schanz², A. Schröder^{1,2}

¹Brandenburg University of Technology, Dep. of Image Based Measurement Techniques, Cottbus, Germany

²German Aerospace Center (DLR), Inst. of Aerodynamics and Flow Technology, Göttingen, Germany
*buchwald@b-tu.de

Abstract

In order to derive accurate acceleration statistics from experiments involving Lagrangian Particle Tracking, it is essential to filter the position noise from the tracks. The ‘TrackFit’ filter is especially well-suited for this task. However, this filter is predicated on the estimation of temporal filter parameters from a model of the global amplitude spectral density of the measured tracks. Consequently, its effectiveness is diminished in inhomogeneous flows with a large range of acceleration variances depending on local flow regions (e.g. free turbulent jets in quiescent fluid). This paper presents a methodology for the automatic determination of requisite filter parameters at a local level, employing the local mean acceleration variance. This approach enables the utilization of the merits of the Trackfit approach, particularly its autonomy from track length and its efficacious noise suppression even in the high frequency band, in statistically stationary, inhomogeneous (turbulent) flows. The results of an experimental study of a round turbulent jet in air utilizing helium-filled soap bubbles illuminated by LED arrays as tracer particles demonstrate the potential of the presented TrackFit version to outperform conventional polynomial-based filters, such as Savitzky-Golay, in an unparalleled range of fluid flows.

1 Introduction

A significant challenge encountered in the field of Lagrangian Particle Tracking (LPT) is the management of measurement noise. The noise has a variety of origins, including camera sensor noise, the limited time sampling of the tracks, or the presence of overlapping particles. To mitigate these effects, modern LPT techniques use filters to smooth derived tracks. Techniques based on polynomial regression, such as the Savitzky-Golay filter, are often used for this purpose. These filters convolve a polynomial of a given length with the measured signal to obtain the smoothed track. Another approach called ‘TrackFit’ (Gesemann et al., 2016; Gesemann 2021) is based on a B-Spline representation of tracks and approximates an optimal Wiener filter by solving an overdetermined linear system of equations derived from the positional data of a track and suitably chosen weights. Both classes of filters rely on effective parameterization to achieve optimal noise suppression. In the context of polynomial filters, the ‘guts feeling’ of experts is frequently employed. For TrackFit on the other hand, Gesemann et al. (2016) presented a physically motivated approach, which enables a determination of the optimal filter parameter based on an analysis of the amplitude spectral density (ASD) of position spectra of reconstructed tracks in an a posteriori manner by querying its cutoff frequency discriminating the signal from noise. The preceding filter methods utilize constant filter parameters for the entire measurement volume, despite the fact that a certain component of the noise evidently varies locally. However, the advent of LPT methods such as Variable-Timestep-Shake-The-Box (VT-STB) (Schanz et al., 2021) has enabled precise measurements of highly inhomogeneous flows. This development underscores the importance of the development of track filtering methods which also suppress noise accurately in highly varying flow and

in regions of very small particle displacements. It follows that approaches should aim at deriving adequate filter parameters based on local flow conditions. In the case of polynomial filters, Janke and Michaelis (2021) proposed an adaptive track filtering approach for polynomial filters, wherein the filter length is determined based on the standard deviation of the particle positions calculated by a polynomial regression. However, polynomial filters are unable to effectively suppress high-frequency noise, regardless of the specific filter parameters employed (Gesemann, 2021; Schmid et al., 2022). This is particularly problematic when information from derivatives of the fitted track is required, as is the case with velocity and acceleration. TrackFit has been shown to be less susceptible to this problem when appropriate weights are selected (Gesemann, 2021; Lawson et al., 2018). K  chler et al. (2024) proposed a methodology for determining the filter parameters for a B-spline based approach, founded upon the analysis of the acceleration variance. Although this approach can, in principle, also be used for a determination adapted to the flow, this would necessitate frequent fitting and subsequent statistical evaluation. We therefore use another approach. The present paper proposes a methodology based on the approach of Gesemann et al. (2016) for the automatic determination of the requisite filter parameter at the local level, employing the local mean acceleration variance. The proposed method enables precise determination of the acceleration in statistically stationary, inhomogeneous flows. The ASDs and measurement results presented are derived from an experimental study of a round turbulent jet in air, utilizing helium-filled soap bubbles (HFSBs) illuminated by LED arrays as tracer particles, which is discussed in the second section. This is followed by a description of the local adaptation of TrackFit in STB and VT-STB experiments and the method's inherent ability to determine positional accuracy. The fourth section is devoted to the discussion and comparison of the results from the original and adapted TrackFit method. To provide a method to generate local filter parameters even in instationary flows, an alternative method is presented as an outlook.

2 Experiment

The experiment was conducted in a large test room measuring $6 \times 4 \times 3.4 \text{ m}^3 = 82 \text{ m}^3$, with blackened walls on three sides and a tent-like ceiling (crest height at $\sim 4 \text{ m}$ along 6 m) made of black cloth as shown in Figure 1 (left). Air was expelled horizontally at a velocity of $U_j = 49.75 \text{ m/s}$ and a height of $\sim 1.25 \text{ m}$ above the floor at the measurement position using a circular contraction nozzle with a diameter of $d = 10 \text{ mm}$, resulting in a Reynolds number of $Re_d = 33,000$. Prior to recording, the room was filled with submillimeter sized ($d_p = 350 \text{ }\mu\text{m}$) HFSBs. The HFSBs were illuminated by a large array of LEDs on the floor ($1.6 \times 1.6 \text{ m}^2$ with a round aperture of 1.25 m diameter) and a smaller one on the ceiling. To increase the reconstructable particle concentration, a scanning approach was applied, where the two halves of the LED array were operated alternately (see Schanz et al., 2024). The LEDs were pulsed at the same frequency as the camera system. The camera system consisted of four v2640 and one v1840 cameras, which recorded $2 \times 6,294$ consecutive images per run. The cameras were located outside the room behind a polycarbonate glass wall. Figure 1 (right) illustrates the positioning and field of view (FOV) of each camera. The three innermost cameras were equipped with $f = 50 \text{ mm}$ Zeiss Planar lenses, while the outermost cameras were fitted with $f = 60 \text{ mm}$ Zeiss Macro Planar lenses. The LEDs and cameras were synchronized at a frequency of $2 \times 1 \text{ kHz}$ for the FOV spanning approximately 160 to 240 nozzle diameters. An alternative field of view (FOV) closer to the nozzle exit was also examined at twice the recording frequency. A comprehensive account of the experimental procedures and the resultant measurements is available in Buchwald et al. (2024). Figure 2 presents an impression of the instantaneous measured streamwise velocity and Q-value field.

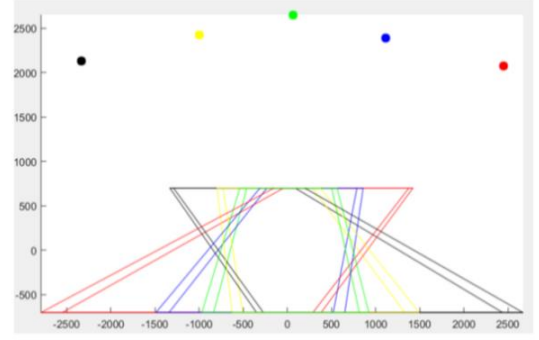


Figure 1: Experimental setup. Left: 82 m^3 test room with LED arrays illuminating the test section, the cylindrical STB measurement volume and a $d = 10 \text{ mm}$ nozzle. Right: top view of calibrated camera system, showing the common illuminated volume of $\sim 1.85 \text{ m}^3$

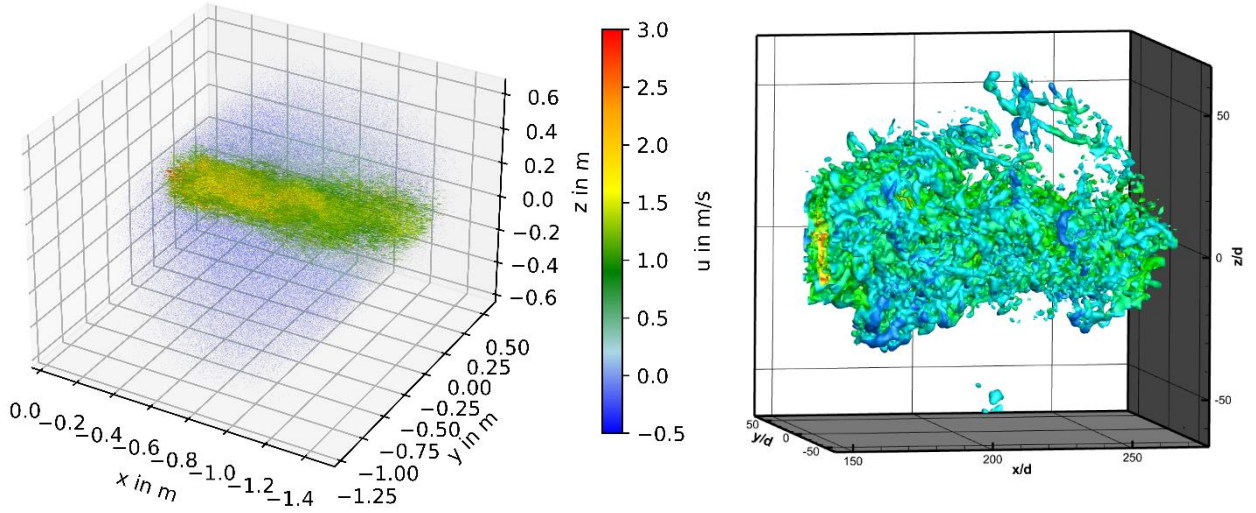


Figure 2: Particle tracks over 20 time-steps (left) and Q -value iso-surfaces of 1800 s^{-2} (right) obtained from FlowFit3 data assimilation (Godbersen et al., 2024), both color-coded by streamwise velocity.

3 Method

Gesemann's (2021) TrackFit methodology is a theoretical framework based on a model of the mean ASD of tracks in turbulent flows. As shown in Figure 3, the modelled ASD comprises two distinct regions. The former is characterised by a $1 / f^3$ decrease, while the latter is characterised by a constant amplitude and is denoted as white noise. The model is utilized to determine a cutoff frequency, which is then employed as a parameterisation for TrackFit. Moreover, the height of the plateau is equivalent to the standard deviation of the position, so the uncertainty of the LPT measurement including 3D reconstruction is also determined a posteriori. However, it is important to note that signal strength is associated with the intensity or Reynolds number of turbulence and thus from its local temporal scale separation and specific spectral content. Consequently, the cutoff frequency is predicted to vary depending on the specific location, which is demonstrated on the right plot of Figure 4. To address this challenge, the original approach is expanded by determining local cutoff frequencies instead of a global one. This approach provides the foundation for calculating the weights that are subsequently used to filter the tracks.

As a preliminary measure, it is imperative to perform an STB evaluation with a presumed cutoff frequency. On the one hand, this cutoff frequency is required to predict the tracks within the STB and VT-STB algorithm; on the other hand, the tracks need to be filtered to enable a better determination of the acceleration variance. This is necessary because the measurement volume is divided into segments based on this measure in the next step. The selection of acceleration variance as the primary indicator is based on its demonstrated efficacy in reflecting the magnitude of the signal component within ASDs. A methodological segmentation strategy utilizing K-means clustering was executed, guaranteeing that each segment comprises approximately an equal quantity of tracks. In this manner, the acceleration variance consistently alters per segment, ensuring a clear separation between signal and noise within each segment. Each segment comprises bins of different acceleration variances, the mean value of which serves as the segment's designation.

Figure 4 shows the segmentation process and respective ASDs of two segments. As is evident, the plateau is separated more clearly in both presented segments than in the global ASD. As the calculation of acceleration used for the segmentation process is derived from a preliminary fitting based on the global cutoff frequency, poorly defined acceleration variance values are present in regions that deviate significantly from the average flow conditions. Consequently, incorporating velocity information, which is less susceptible to noise, may be necessary for the construction of segments.

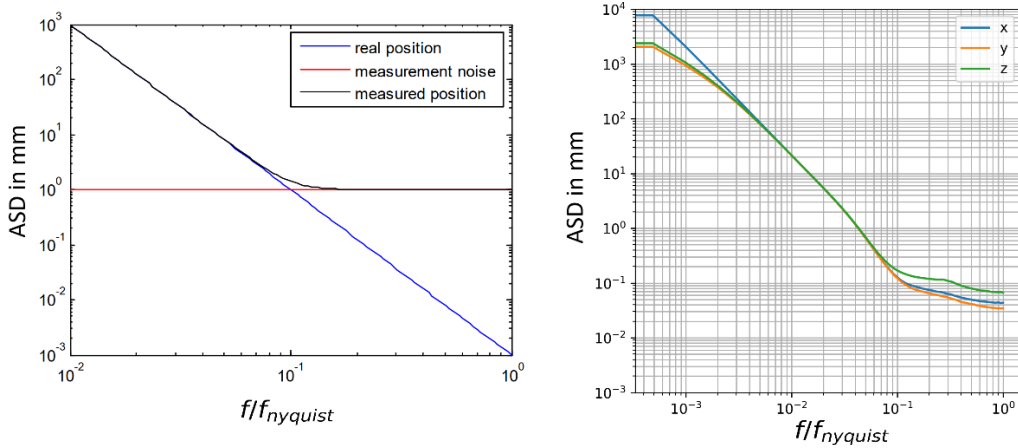


Figure 3: Model of the ASD of particle motion for arbitrary turbulent flow (left, adapted from Gesemann et al. (2016)), and measured global ASD of all position components in a strongly inhomogeneous jet flow (right).

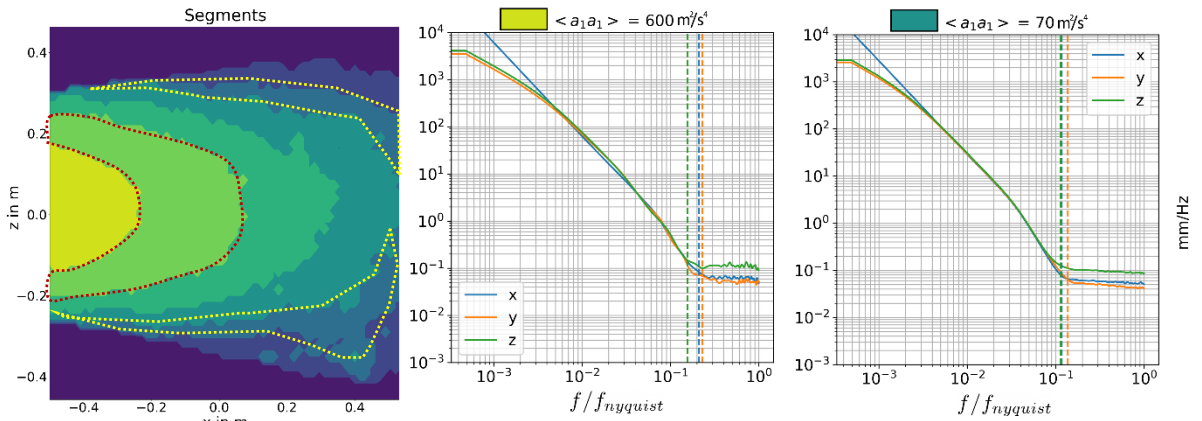


Figure 4: Segments with different mean ensemble-averaged acceleration variance in the xz-plane at $y=0$ of a turbulent jet (left) along with the corresponding ASDs of two exemplary segments. The dashed lines mark automatically determined cutoff frequencies.

In our case, we observed an unphysical (excessive) acceleration variance at outer more quiescent regions of the flow and in the edges of the measurement volume. However, these values were still classified within the segment with the lowest mean acceleration variance. After computing the spatial distribution of the cutoff frequencies, the tracks can be fitted locally. It is possible to assign a specific cutoff frequency to each position for each point in time. Alternatively, the tracks can be cut into sections where the cutoff frequency remains constant. The latter approach requires less implementation effort and is the foundation for the presented results.

As the height of the plateau of the ASD is indicative of the standard deviation of position, the positional accuracy of particles in the raw tracks can also be determined for each segment. Consequently, the influence of noise on the central moments of velocity and acceleration computed from raw tracks can be calculated by linear error propagation, as asserted in (Gesemann, 2021). By interpolating between the segments, the measurement can be adjusted for the influence of image and 3D reconstruction noise in the entire measurement volume for each of these variables.

The local determination of the TrackFit filter weights is of particular relevance in highly inhomogeneous flows. To achieve accurate particle tracking under these conditions, VT-STB has been developed (Schanz et al., 2021). In VT-STB, the time separation is varied by omitting a certain number of images from the dataset for the evaluation. In the following, the step width in the dataset employed for evaluation is referred to as time-step width Δ_t . The evaluation starts with a time-step width such that the slowest particles of the flow can be optimally tracked. From there, the time-step width is iteratively reduced, while feeding the particles tracked within the previous iterations. Finally, the original time-separation of the recording, corresponding to a time step width $\Delta_t = 1$, is reached, where only the fastest or most accelerated particles remain to be tracked. Given the inhomogeneous nature of turbulent jets, the VT-STB evaluation method was employed for the purpose of analysis. To undertake this process, it is first necessary to select the time step widths. The objective here is to ensure that there is a suitable time step width for each flow region in the measurement volume, in which the tracks in this region are found. Therefore, the time step width should not vary too much between successive iterations. As a result, often multiple time-step widths are suitable for the cutoff frequency determination of a single segment.

4 Results and Discussion

To determine from which pass, i.e. with which time-step width, the cutoff frequency in a specific segment should be determined, it is beneficial to examine the corresponding ASDs in different time-step widths. As demonstrated in Figure 5, the cutoff frequencies and noise for segments $\langle a_1 a_1 \rangle = 100 \text{ m}^2/\text{s}^4$ and $\langle a_1 a_1 \rangle = 260 \text{ m}^2/\text{s}^4$ are clearly distinguishable in both time-step widths. The X-axis is scaled by the Nyquist frequency corresponding to each evaluation. As the Nyquist frequency is half the sampling frequency, comparing the cutoff frequencies requires a factor based on the relationship between the sampling frequencies, which, in this case, is a factor of two.

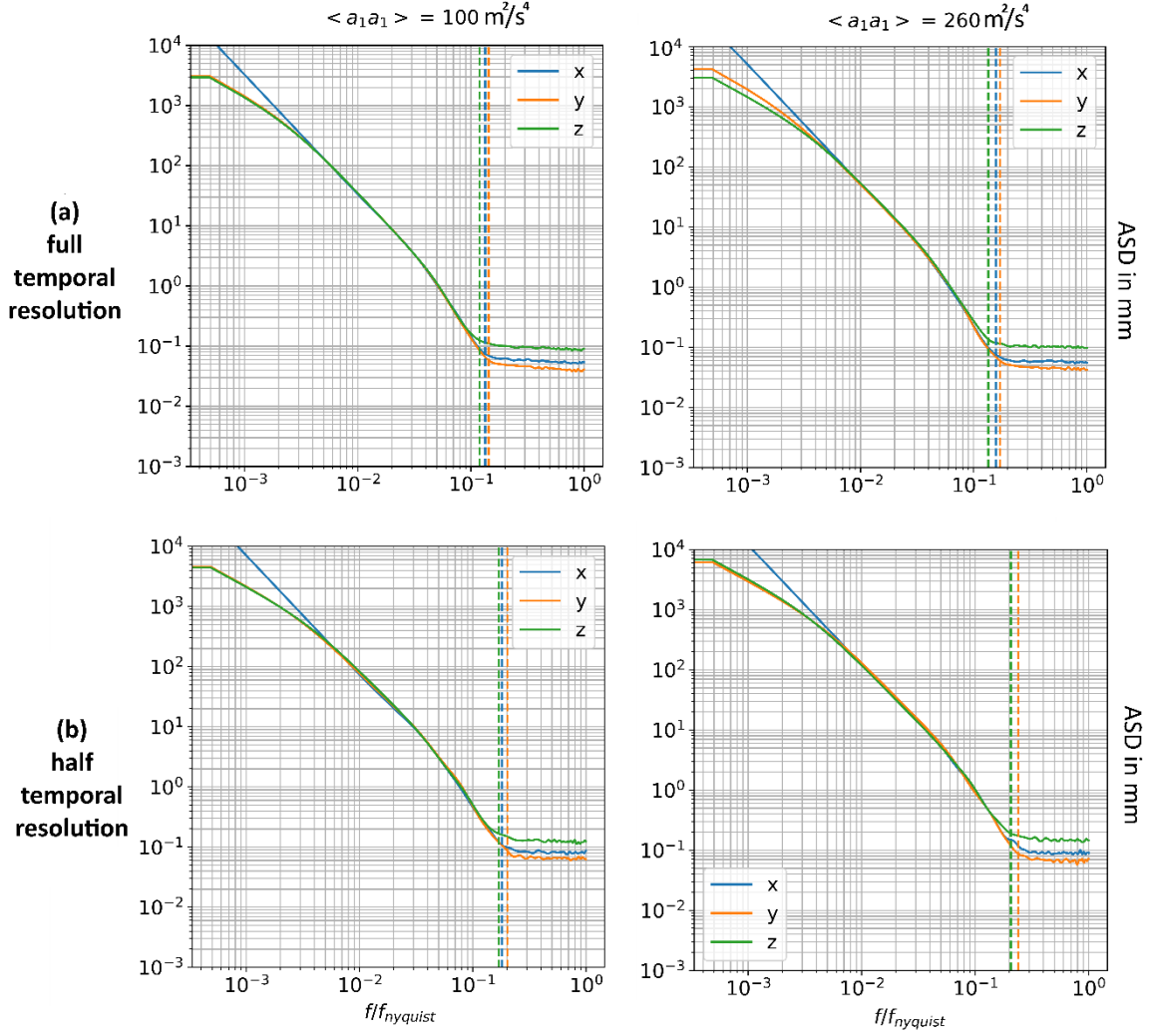


Figure 5: ASDs obtained from passes with time-step width $\Delta_t = 1$ (a) and $\Delta_t = 2$ (b) for two segments.

One advantage of VT-STB is that it allows customized STB parameters for each pass, fine-tuning the tracking parameters to the different flow regimes tracked in each iteration. Consequentially, variations in noise and converted cutoff frequency are to be expected. Table 1 presents the ratio of noise and converted cutoff frequencies for three segments of intermediate turbulence intensities, in which a reliable determination between two different time-step widths was possible. The cutoff frequency was determined by taking 1.3 times the noise plateau as the dividing line. The noise consistently exhibits a higher amplitude when the time-step width is doubled. This observation is consistent with the finding that the converted cutoff frequency is lower, leading to optimal filter weights that yield a filter with a broader frequency suppression range. The findings demonstrate that when fitting the tracks, it is imperative to consider not only their spatial coordinates, but also the employed time-step width.

Pass ($\Delta_t = 2$) / Pass($\Delta_t = 1$)	f_{co} (x)	f_{co} (y)	f_{co} (z)	σ_x	σ_y	σ_z
Segment: 260 m ² /s ⁴	0.76	0.7	0.77	1.55	1.47	1.4
Segment: 100 m ² /s ⁴	0.68	0.7	0.71	1.44	1.47	1.34
Segment: 43 m ² /s ⁴	0.81	0.7	0.75	1.39	1.47	1.31

Table 1: Relation of (converted) cutoff frequencies (f_{co}) and position noise σ according to ASDs from VT-STB passes with time increments $\Delta_t = 1$ (full temporal resolution) and $\Delta_t = 2$ (half temporal resolution).

The subsequent results are derived from an evaluation in which all tracks originate from the final pass using full time resolution. However, it is important to acknowledge that a considerable number of these tracks had previously been identified in passes with a higher time-step width. These tracks were then utilized to initiate the final pass. In the final pass, these previously identified tracks undergo a subsequent adjustment via shaking. Consequently, the cut off frequencies for fitting stem from a test pass with full time resolution for all segments in which this was feasible. In all other segments, the cutoff frequencies are computed by taking the results from passes with half or eighth temporal resolution and multiplying them by the relation of the respective sampling frequencies to the full resolution.

The comparison of the radially averaged profiles of velocity variance $\langle uu \rangle$ and acceleration variance $\langle a_1 a_1 \rangle$ utilizing global and locally adapted TrackFit is illustrated in Figure 6. Although the velocity variance profile exhibits minimal variation, it is apparent that the original TrackFit induces a significant, non-physical increase in acceleration variance toward the periphery of the measurement volume. This phenomenon can be attributed to the fact that particles exhibit minimal movement between two frames in these regions, such that the measured accelerations are dominated by image noise. Since the used cutoff frequency is larger than the ‘real’ one for these regions, a considerable part of this noise is not filtered. In contrast, the locally adapted Trackfit demonstrates more plausible, self-similar acceleration variance profiles.

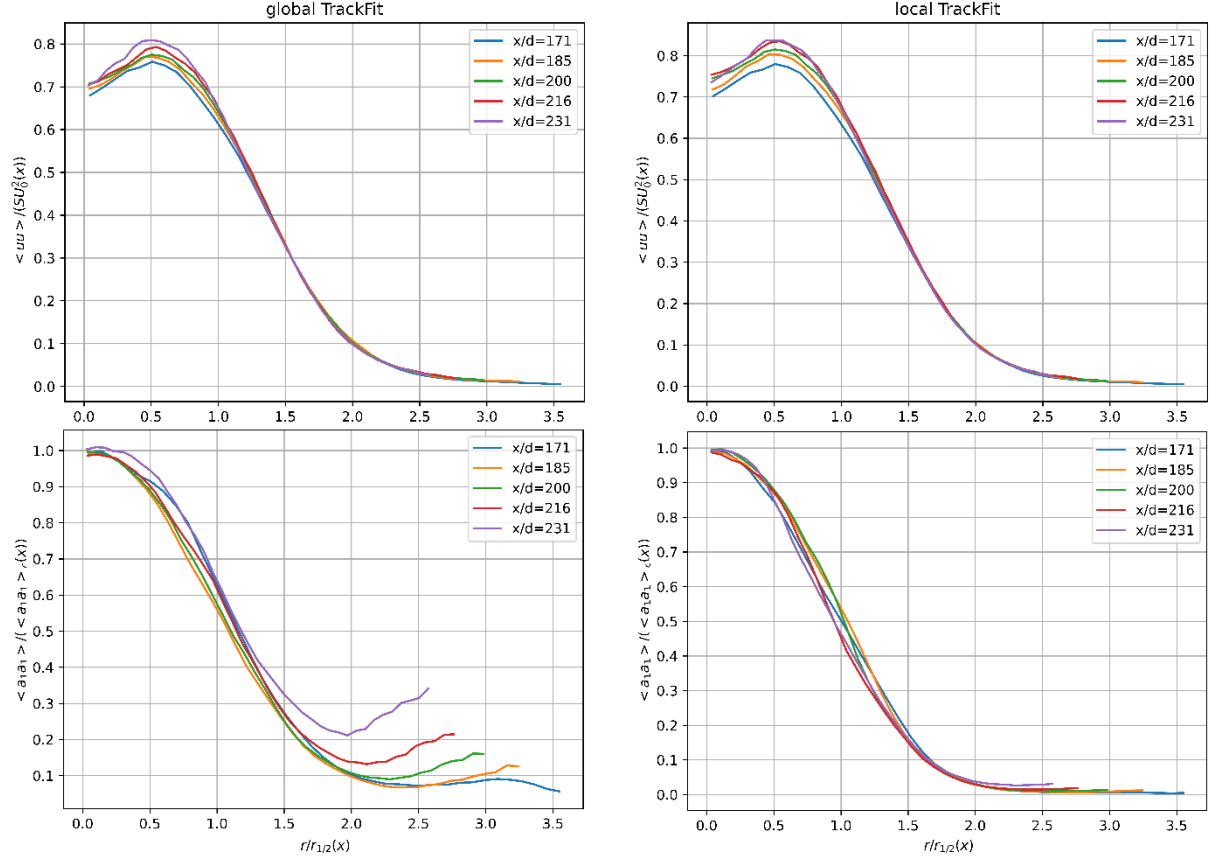


Figure 6: Radially averaged profiles of the x-component of ensemble averaged velocity variance $\langle uu \rangle$ and acceleration variance $\langle a_1 a_1 \rangle$ at a specific distance x/d from the nozzle using global and local filtering (left and right). The x-axis is scaled by the half-width $r_{1/2}$. The Y-axis of velocity variance plots is scaled by the spreading rate S and mean centerline velocity U_0 . The Y-axis of acceleration variance is only scaled by its centerline value.

5 Conclusion and outlook

In this study, a methodology was proposed for the automatic extraction of filter parameters for TrackFit from multiple passes with varying time-step widths in a VT-STB evaluation. This approach enables utilization of the merits of TrackFit, particularly its autonomy from track length and its efficacious noise suppression even in the high frequency band, in stationary, inhomogeneous flows.

A comparison was made between the fitting results of a large-scale turbulent round jet dataset utilizing global and the presented locally adapted Trackfit. It was revealed that the global method yields unphysical acceleration profiles in the more quiescent periphery of the jet, while the local one shows self-similar profiles. It is suggested by these results that the local filter parameter determination significantly mitigates the acceleration error, particularly in slow regions. Moreover, the experimental findings reveal that the acceleration profiles in the far field of a turbulent jet exhibit self-similar characteristics, a novel observation to the best of the authors' knowledge. The results suggest that it is reasonable to assume that the superiority of Trackfit over conventional polynomial filters such as Savitzky-Golay, which has already been demonstrated in spectral space (Gesemann, 2021), can be extended to an unprecedented range of fluid flows with the aid of local determination of filter parameters. An in-depth comparison of the filter's performance against Savitzky-Golay not only in spectral space but also by comparison with ground truth values using a synthetic experiment will be the subject of a subsequent publication.

The presented procedure can also be used to improve the prediction of particle positions carried out in STB, as this is also dependent on a determination of cutoff frequencies which are used to compute the filter parameters. A further advantage of the procedure presented is the possibility of using the ASDs obtained from various passes to draw conclusions as to whether the selected time-step widths and the set of STB parameters used are suitable.

Furthermore, local TrackFit is conceptually uncomplicated; however, it fails to consider the fact that tracks within a segment can possess vastly different properties. In addition, substantial variations in flow conditions are observed even within individual tracks. Consequently, the computed weights, as determined by the local TrackFit approach, demonstrate a clear opportunity for further optimization. Additionally, the current approach is not designed to handle unsteady flows. Therefore, an extension to the approach is currently being developed, in which a filter weight is assigned to each individual particle in each time step. Achieving this objective requires the development of a function that maps the local acceleration to a corresponding cutoff frequency.

Acknowledgement

We thank Chris Willert and Michael Schroll from DLR, AT-OTM, Cologne for providing the round jet. We also express our gratitude to Abhijna Raghava Simhan and Hemanth Naidu Kotra for their contributions in setting up the experiment.

References

Buchwald T, Godbersen P, Schanz D, and Schröder A (2024) Large scale turbulent round free jet far field investigations using Shake-The-Box 3D Lagrangian particle tracking. In *21st Symposium on Applications of Laser Techniques to Fluid Mechanics*, Lisbon, Portugal

Gesemann S (2021) TrackFit: Uncertainty quantification, optimal filtering and interpolation of tracks for time-resolved Lagrangian particle tracking. In *14th International Symposium on Particle Image Velocimetry*, Chicago, IL

Gesemann S, Huhn F, Schanz D, and Schroder A (2016) From noisy particle tracks to velocity, acceleration and pressure fields using b-splines and penalties. In *18th international symposium on applications of laser and imaging techniques to fluid mechanics*, Lisbon, Portugal

Godbersen P, Gesemann S, Schanz D, and Schröder A (2024) FlowFit3: Efficient data assimilation of LPT measurements. In *21st International Symposium on Applications of Laser and Imaging Techniques to Fluid Mechanics*, 08 - 11 July 2024, Lisbon, Portugal.

Janke T and Michaelis D (2021) Uncertainty quantification for PTV/LPT data and adaptive track filtering. In *14th International Symposium on Particle Image Velocimetry*, Chicago, IL

Küchler C, Ibanez Landeta A, Moláček J, and Bodenschatz E (2024) Lagrangian particle tracking at large Reynolds numbers. *Review of Scientific Instruments* 95(10):105110. <https://doi.org/10.1063/5.0211508>

Lawson JM, Bodenschatz E, Lalescu CC, and Wilczek M (2018) Bias in particle tracking acceleration measurement. *Experiments in Fluids* 59:172. <https://doi.org/10.1007/s00348-018-2622-0>

Schanz, D, Schröder, A, Bosbach, J, Strübing, T, Wolf, C, Schwarz, C and Heintz, A. (2024). Scanning Lagrangian Particle Tracking to measure 3D large scale aerodynamics of quadcopter flight. In *21st International Symposium on Applications of Laser and Imaging Techniques to Fluid Mechanics*, 08 - 11 July 2024, Lisbon, Portugal.

Schanz D, Novara M, and Schröder A (2021) Shake-The-Box particle tracking with variable time-steps in flows with high velocity range (VT-STB). In *14th International Symposium on Particle Image Velocimetry*, Chicago, IL

Schmid M, Rath D, and Diebold U (2022) Why and how Savitzky–Golay filters should be replaced. *ACS Measurement Science Au* 2(2):185–196. <https://doi.org/10.1021/acsmeasuresciau.1c00054>